Contents lists available at Science-Gate

International Journal of Advanced and Applied Sciences

Journal homepage: http://www.science-gate.com/IJAAS.html

# Pounding response of two adjacent planar structures with different floor levels due to earthquake excitation using the finite element method

Hoa P. Hoang [1], Trung D. Pham [2,*], Hien M. Le [2], Phuoc T. Nguyen [3]

[1]*Faculty of Road and Bridge Engineering, Da Nang University of Science and Technology, Da Nang, Vietnam*
[2]*Department of Civil Engineering, Mientrung University of Civil Engineering, Tuy Hoa City, Vietnam*
[3]*Department of Civil Engineering, Ho Chi Minh City Open University, Ho Chi Minh City, Vietnam*

ARTICLE INFO

*Article history:*
Received 2 March 2020
Received in revised form
1 July 2020
Accepted 15 July 2020

*Keywords:*
Adjacent structures
Earthquake-induced pounding
Different floor levels
Impact force
Finite element method

ABSTRACT

Recently, dynamic excitation loads often cause damages in the adjacent structures with different dynamic characters through the pounding effect. This study analyzes the pounding response of the two adjacent structures with different floor levels associated with earthquake excitation. The structure system model was built based on the finite element method, and the governing equation of the structure system motion was established based on the dynamic balancing principle and solved by the New mark method in the time domain. The results indicate that the characteristic parameters significantly affect the dynamic response of the structure system. This study also shows that the pounding effect causes damages to the adjacent structure.



## 1. Introduction

Under dynamic loads, adjacent structures can be suffered from a pounding effect when the gap between the two structures is not large enough. Especially, adjacent structures with different dynamic characters will likely experience a pounding effect during earthquake events (Anagnostopoulos and Spiliopoulos, 1992). This pounding effect during an earthquake is one of the main reasons causing 20% to 30% of structural destruction (Anagnostopoulos, 1988). For example, about 15% of total collapsed buildings were related to structural pounding in the 1985 Mexico earthquake (Rosenblueth and Meli, 1986; Anagnostopoulos, 1994). Researchers also showed that pounding-related damage was more than 200 out of 500 damaged buildings in San Francisco, Oakland, Santa Cruz, and Watsonville during the Loma Prieta earthquake in 1989 (Kasai and Maison, 1997). Therefore, numerous studies on pounding response in adjacent structures during an earthquake have been conducted during the last two decades (Ruangrassamee and Kawashima, 2001; Chau et al., 2004; Agarwal et al., 2007; Jankowski, 2005a; 2005b; 2006a; 2006b; 2007; 2008; 2010; Hameed et al., 2012; Mahmoud et al., 2012; 2013; Efraimiadou et al., 2013a; 2013b; Raheem, 2014; López-Almansa and Kharazian, 2014; Mattia et al., 2015; Kumar and Karuna, 2015; Naderpour et al., 2016; Liu et al., 2017; Li et al., 2017; Namboothiri, 2017; Tubaldi et al., 2012; Trung et al., 2018). However, most of the above studies only focused on equal-height storeys or idealized as the lumped mass model.

In addition, other studies on the pounding response of the adjacent structures with different storey heights subjected to earthquake-induced pounding. For example, Karayannis and Favvata (2005) and Favvata et al. (2013) investigated the pounding response of two adjacent reinforced concrete structures with non-equal heights idealized as lumped mass models. Efraimiadou et al. (2012) and Hatzigeorgiou and Pnevmatikos (2014) studied the linear behavior of adjacent planar reinforced concrete frames subjected to strong ground motions by applying for the RUAUMOKO program. They showed that vertical ground motion mildly affects the seismic response of adjacent buildings subjected to structural pounding. However, the structural damage was moderately affected by the vertical component of earthquakes.

In this study, a linear viscous elastic model was employed to investigate the pounding response of two adjacent planar structures due to earthquake excitation. One important contribution of this study is the finite element model for planar structures with different floor levels subjected to earthquake-

* Corresponding Author.
Email Address: phamdinhtrung@muce.edu.vn (T. D. Pham)
https://doi.org/10.21833/ijaas.2020.12.003
Corresponding author's ORCID profile:
https://orcid.org/0000-0001-8629-0640

induced pounding, which was completely disjointed. The pounding element with the pounding force was simulated by applying the linear viscoelastic elements for each storey of each structure. The governing equation of motion of the structure system was established based on the dynamic balancing principle and solved by the new mark method in the time domain. Finally, characteristic parameters of the structure system, such as the gap between two adjacent structures, the different floor levels, and the ground acceleration, were investigated in detail.

## 2. Structural pounding model

Most of the other studies (Jankowski and Mahmoud, 2015) showed that there were two typical approaches to simulate structural pounding due to earthquakes. The first approach was considered as the classical theory of impact bases on the laws of conservation of energy and momentum. However, this approach does not consider stresses and deformations in the colliding structural elements during impact. Experimental studies proved that this approach was not recommended to structures modeled as multi-degree-of-freedom systems or the study on the pounding of adjacent buildings, or between segments of a bridge.

The second approach is based on the direct model of impact force during a collision with the time history of pounding force during impact. This approach consists of two phases: Approach period and restitution period. By using elastic or viscoelastic impact elements (including linear elastic model, linear viscous elastic model, modified linear viscous elastic model, Hertz non-linear elastic model, Hertzdamp non-linear model, and non-linear viscoelastic model), these above limitations were handled. In addition, experimental results indicated that the efficiency of these models depends on the type of analysis conducted, the application of the linear viscoelastic, and the Hertzdamp. The non-linear viscoelastic models also give the smallest errors in the time history of the dynamic response of the example structures due to earthquake-induced pounding (Jankowski and Mahmoud, 2015).

Hence, the linear viscous elastic model consists of a linear spring with the addition of linear damper was used in this study to simulate the pounding force during impact at the time $t$, and can be expressed as follows (Anagnostopoulos, 1988; 2004; Komodromos et al., 2007; Jankowski and Mahmoud, 2015).

$$F_{imp}(t) = k_{imp}\delta(t) + c_{imp}\dot{\delta}(t) \quad (1)$$

where $k_{imp}$ is the impact element's stiffness, $\delta(t)$ denotes the deformation of colliding structural elements, $\dot{\delta}(t)$ describes the relative velocity between colliding structural elements, and $c_{imp}$ denotes the impact element's damping which is given by,

$$c_{imp} = 2\xi\sqrt{k_{imp}\frac{m_1 m_2}{m_1+m_2}} \quad (2)$$

in which $\xi_{imp}$ denotes is the damping ratio related to the coefficient of restitution, expressed as follows:

$$\xi_{imp} = \frac{-\ln COR}{\sqrt{\pi^2+(\ln COR)^2}} \quad (3)$$

with COR is the coefficient of restitution, $m_1$ and $m_2$ denote the mass of two colliding elements, respectively.

## 3. The model of the adjacent structure system due to earthquake-induced pounding

The adjacent structure system disjointed based on the finite element method consists of two different structures with different floor levels subjected earthquake-induced pounding as plotted in Fig. 1.

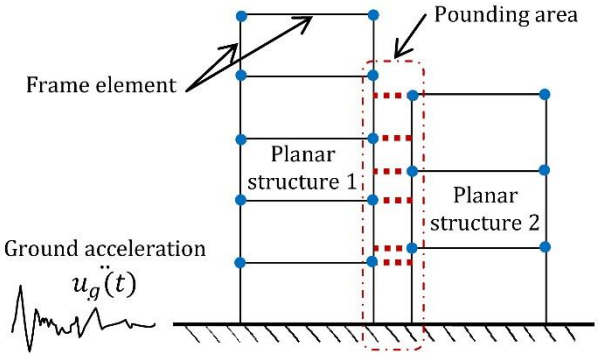


**Fig. 1:** The model of the two adjacent planar structure due to earthquake-induced pounding

It can be seen that between two structures, there is a pounding area where the impact force was applied at any position in the frame elements instead of nodes in the cases of equal floor levels. Therefore, the impact forces in each frame element will be transformed into joint forces and moments at each end of the frame element, see in Fig. 2.

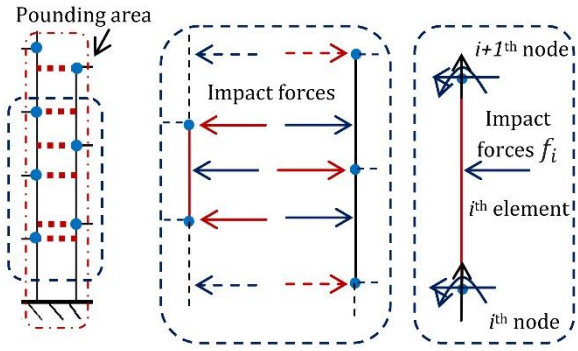


**Fig. 2:** The model of frame element with impact forces

2D-frame element (Fig. 3) was then employed to model the structure. The impact force vectors, the horizontal displacement, and velocity at the pounding joint of each frame element in each planar

structure will also be obtained by using the shape function. Therefore, the characteristic parameters of the linear viscous elastic model are determined in each time step, and the impact force described in the Eq. 1 will also be obtained.

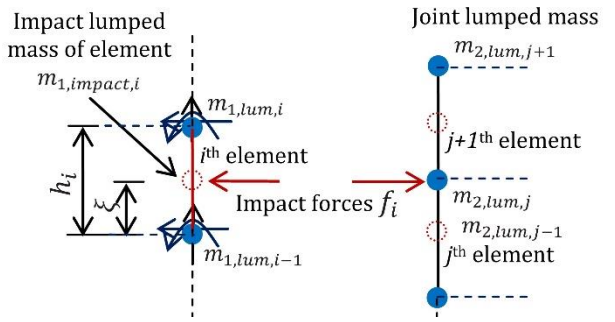


**Fig. 3:** The detail of the impact element

In addition, based on the principle of dynamic balancing and by assembling the frame element matrices and force vectors in the global coordinates, the governing equation of motion of the structure system at the time $t$ can be written as,

$$\mathrm{M}\ddot{u} + \mathrm{C}\dot{u} + \mathrm{K}u = -\mathrm{M}_{lum}\mathrm{D}_{node}\ddot{u_g}(t) + F(t) \quad (4)$$

where $u$ denotes the global displacement vector, $F$ is the global impact force vector, M and K are the global mass and stiffness matrix, respectively, given by,

$$\mathrm{M} = \begin{bmatrix} \mathrm{M}_1 & 0 \\ 0 & \mathrm{M}_2 \end{bmatrix}, \mathrm{K} = \begin{bmatrix} \mathrm{K}_1 & 0 \\ 0 & \mathrm{K}_2 \end{bmatrix}, \mathrm{C} = \begin{bmatrix} \mathrm{C}_1 & 0 \\ 0 & \mathrm{C}_2 \end{bmatrix} \quad (5)$$

in which $\mathrm{M}_i$ ($i = 1, 2$ denotes the planar structure 1 and planar structure 2, respectively) is the global mass of each structure, $\mathrm{K}_i$ is the stiffness matrix of each structure and $\mathrm{C}_i$ denotes the global damping matrix of each structure, obtained by adopting Rayleigh damping as follows

$$\mathrm{C}_i = \alpha_0 \mathrm{M}_i + \alpha_1 \mathrm{K}_i \quad (6)$$

with $\alpha_0$ and $\alpha_1$ denote Rayleigh damping coefficients corresponding with each structure. $\mathrm{M}_{lum}$ denotes the global lumped mass matrix and $\mathrm{D}_{nod}$ is the global position matrix, corresponding with degrees of freedom in horizontal displacement, can be expressed follows as:

$$\mathrm{M}_{lum} = \begin{bmatrix} \mathrm{M}_{lum,1} & 0 \\ 0 & \mathrm{M}_{lum,2} \end{bmatrix}, \mathrm{D}_{nod} = \begin{bmatrix} \mathrm{D}_{nod,1} & 0 \\ 0 & \mathrm{D}_{nod,2} \end{bmatrix} \quad (7)$$

It can be seen that the global matrices in the governing equation of motion of the structure system are invariant matrices, which are not difficult to determine and establish by using the finite element method. But the general impact force vector $F(t)$ during pounding is a variable vector because of the value of impact force depend on velocity and acceleration of the colliding element at each time step, is given by,

$$\mathrm{F} = \begin{bmatrix} \mathrm{F}_1 & \mathrm{F}_2 \end{bmatrix}^{\mathrm{T}} \quad (8)$$

where $F_i$ denotes the global impact force vector of each structure.

The above governing equation of motion of the structure system subjected to earthquake-induced pounding (Eq. 4) is used for studying the dynamic response of the structural system and was solved by direct integration method based on the New mark algorithm, plotted in Fig. 4.

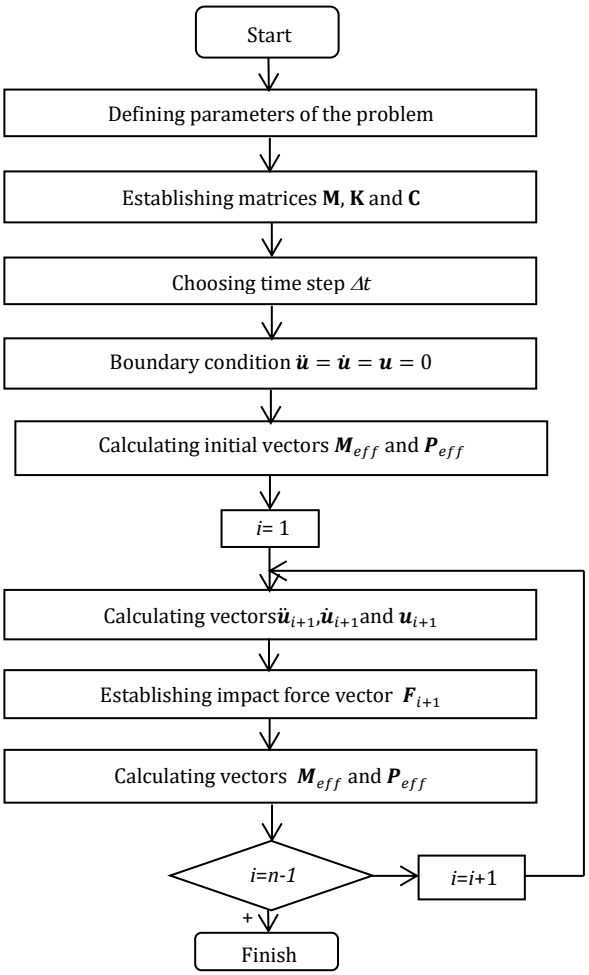


**Fig. 4:** Flowchart for analyzing the dynamic response of the structure system due to earthquake-induced pounding

## 4. Results

In this study, two adjacent concrete buildings (10 and 5 stories) with different floor levels were selected for analysis. Concrete density, $\rho = 2500\ kg/m^3$, Young's modulus $E = 2.7x10^{10} N/m^2$, and the damping ratio $\xi = 0.3$. Two buildings are disjointed based on the finite element method with the as shown in Fig. 5. The pounding model includes the linear viscous elastic model with impact stiffness $k_{imp} = 1.25E6\ kN/m$, and the coefficient of restitution COR = 0.7 (Komodromos et al., 2007). The earthquake excitations vary from weak to strong peak amplitude such as Superstition earthquake, Hachino earthquake, El-Centro earthquake, and San Fernando earthquake, as shown in Fig. 6.

In this section, the height ratio ($\mathrm{Si}_{\mathrm{H}}$) representing the difference of floor levels between the two adjacent structures is defined as the ratio of the first storey height of the planar structure 1 to the first

storey height of the planar structure 2. It assumes that all remain storeys in the system structure are equal height and the range of value of the ratio $Si_H$ varies from 0.5 to 1.5, representing the impact position during nearly the mid-point of the lower storey to the upper storey.

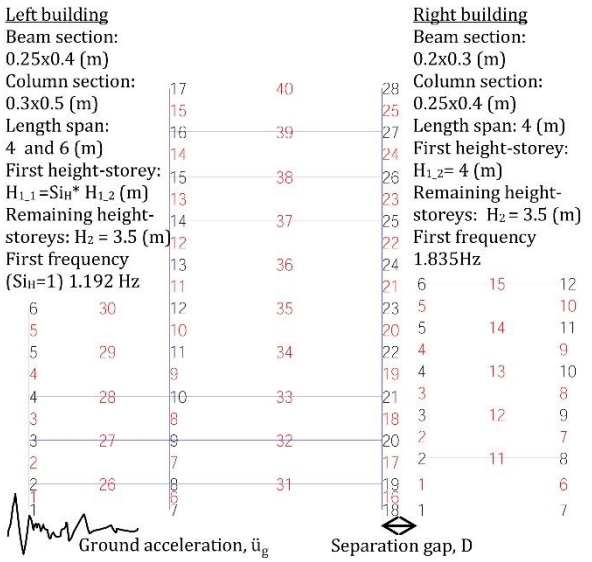


**Fig. 5:** The finite element model of the two adjacent structures with different floor levels

First the effects of height ratio $Si_H$ with different separation, gaps were studied. It can be seen that the pounding effect leads to an increase in the dynamic response of the structure under earthquakes in almost cases. In particular, earthquake-induced pounding.

Increases the peak horizontal displacement of the structures with different separation gap and the height ratio $Si_H$, plotted in Fig. 7 and Fig. 8. However, in some cases, this effect is advantageous for the left building or the right building, and this advantage is not more significant than in the case without the effects of pounding, as shown in Fig. 7 and Fig. 8.

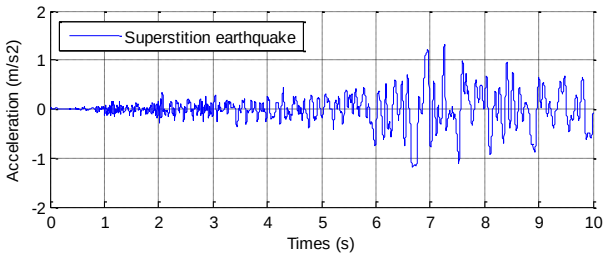


(a)

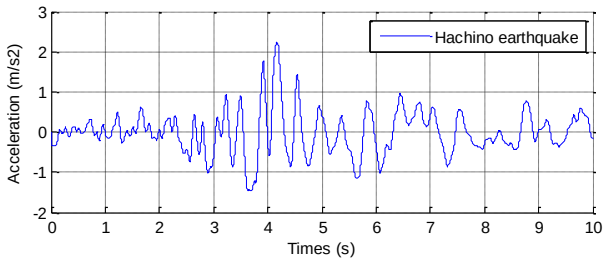


(b)

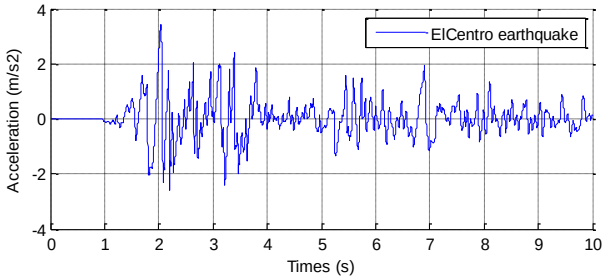


(c)

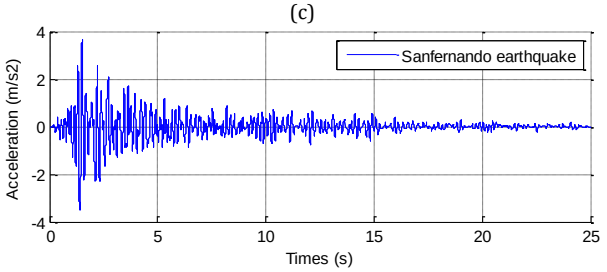


(d)

**Fig. 6:** The time history of ground accelerations: (a) Superstition, (b) Hachino, (c) El-Centro, (d) San Fernando

Although it is useful in some cases, this effect increases the disadvantages significantly on the dynamic response of the structures due to earthquakes. Horizontal displacement decrease when the pounding effect was considered. Especially, these disadvantages are shown clearly when the gaps are not large enough $D = 0.01$ (m) to $D = 0.03$ (m), plotted in Fig. 7 and Fig. 8. In addition, the height ratio $Si_H$ has different influences on the peak displacement of each building with different separation gaps and excitation input. Generally, when the point-impacts occur nearly mid-point column ($Si_H = 0.5$ to 0.75 or $Si_H = 1.25$ to 1.5), horizontal displacement increase comparing to equal floor levels in some earthquakes, as shown in Fig. 7 and Fig. 8.

Additionally, the pounding effect will cause impact forces at the nodes-impact between the two adjacent structures, opposing the horizontal displacement of the nodes-impact in both the structures. Horizontal acceleration of the system structure also increases when the pounding effect is considered, as presented in Fig. 9 and Fig. 10. It can be seen that the increase of accelerations is proportional to the impact force for the different earthquakes. On the other hand, the impact force depends on the separation gaps and ground motion. When the separation gap is relatively small, (0.01 to 0.03m) impact forces are significant (see in Fig. 11 and Fig. 12). In addition to impact force, the shear force also increases significantly when considering pounding in the analysis for some earthquake, as shown in Fig. 13 and Fig. 14.

To show more clearly the effects of the pounding effect on the dynamic response of the system structure, the maximum values at nodes and elements of each building, plotted from Fig. 15 to Fig. 20. It can be seen that the pounding effect also has different influences on the dynamic response of the system structure.

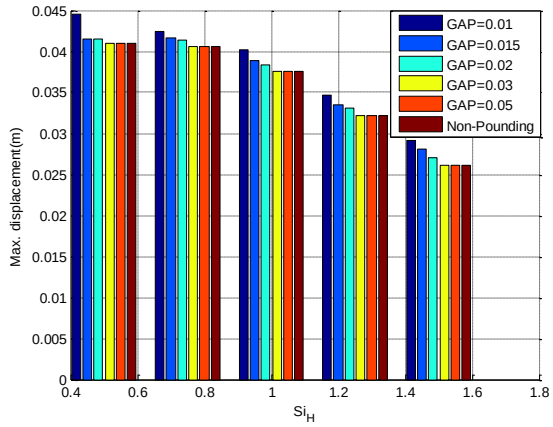


(a)

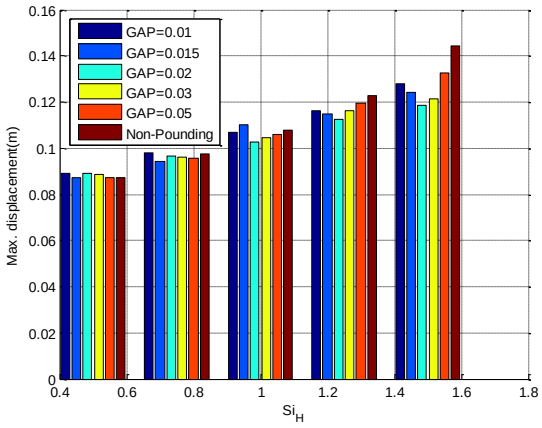


(b)

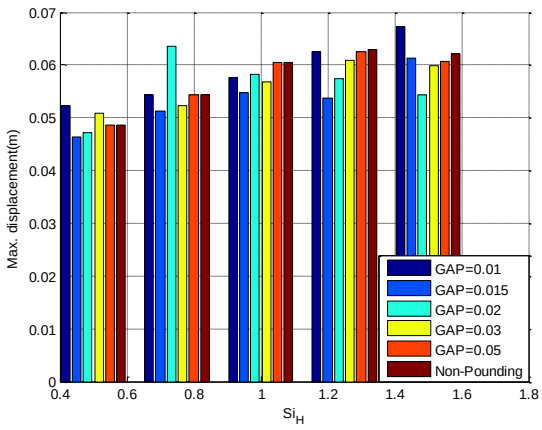


(c)

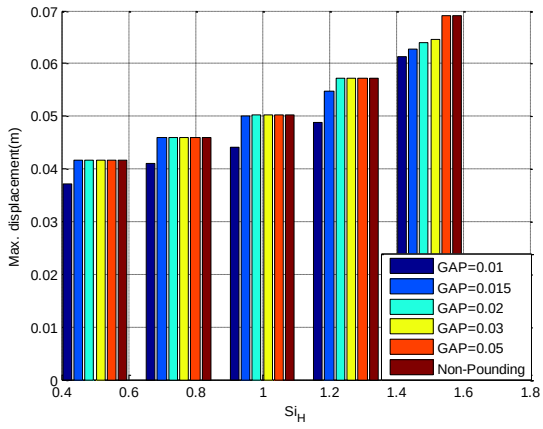


(d)

**Fig. 7:** The effects of $Si_H$ ratio on the maximum horizontal displacement of the left building with different separation gap: (a) Superstition, (b) Hachino, (c) El-Centro, (d) San Fernando

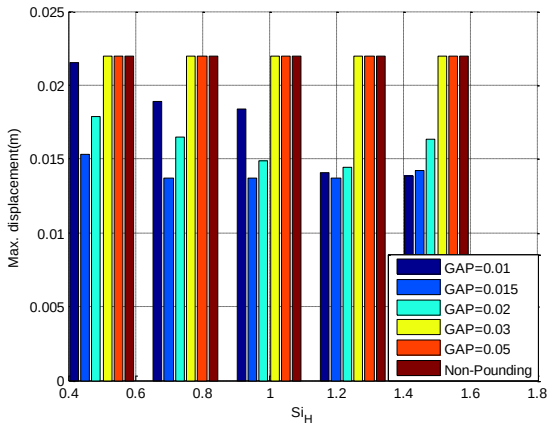


(a)

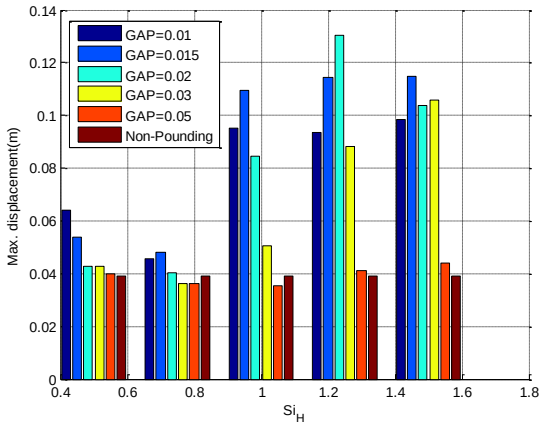


(b)

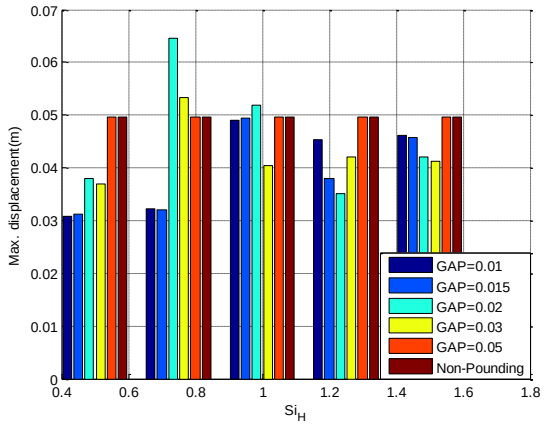


(c)

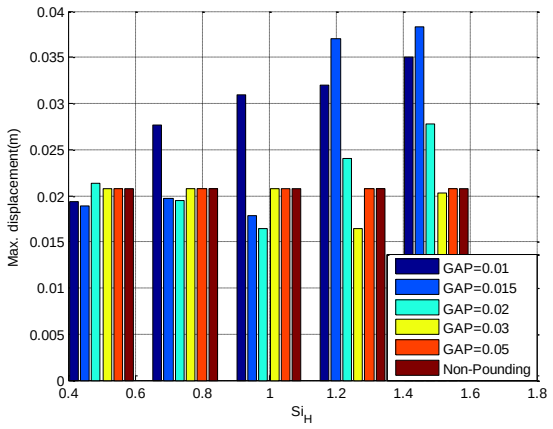


(d)

**Fig. 8:** The effects of $Si_H$ ratio on the maximum horizontal displacement of the right building with different separation gap: (a) Superstition, (b) Hachino, (c) El-Centro, (d) San Fernando

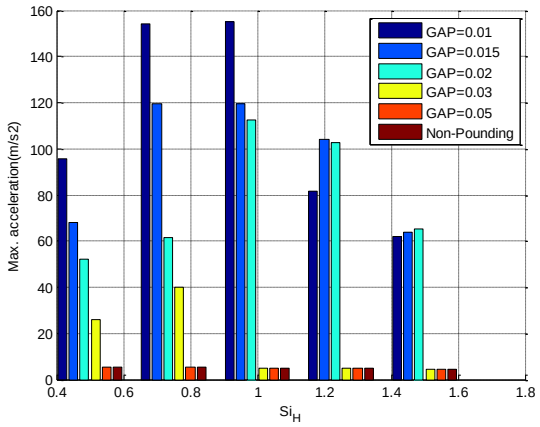


(a)

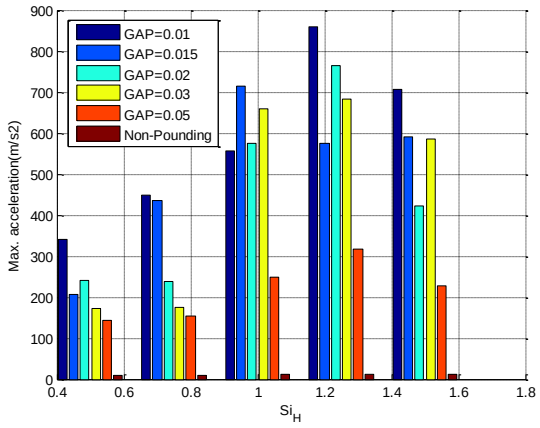


(b)

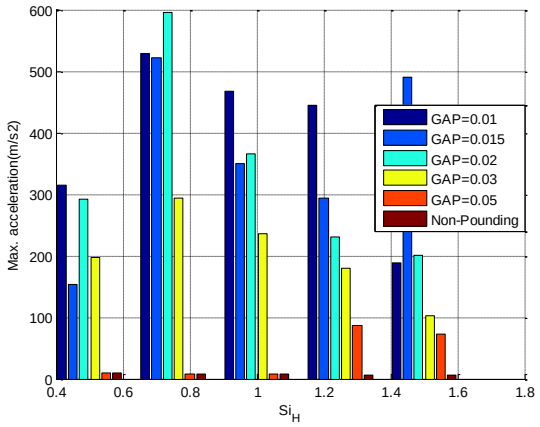


(c)

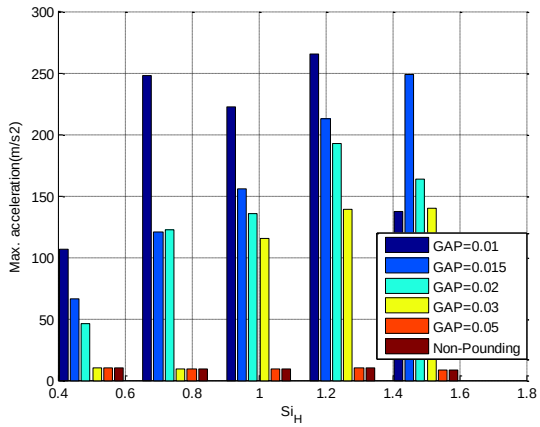


(d)

**Fig. 9:** The effects of $Si_H$ ratio on the maximum horizontal acceleration of left building with different separation gap: (a) Superstition, (b) Hachino, (c) El-Centro, (d) San Fernando

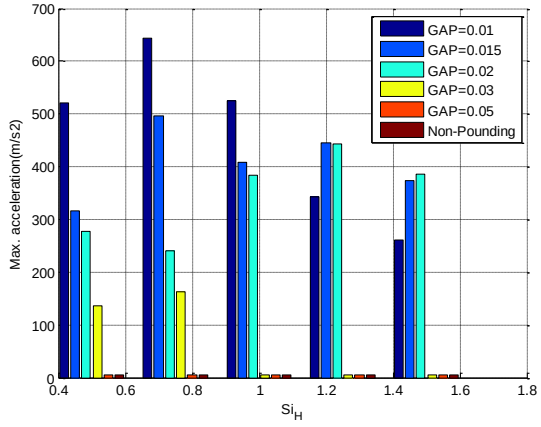


(a)

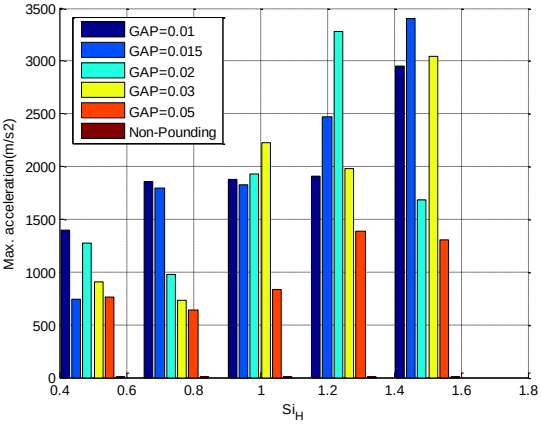


(b)

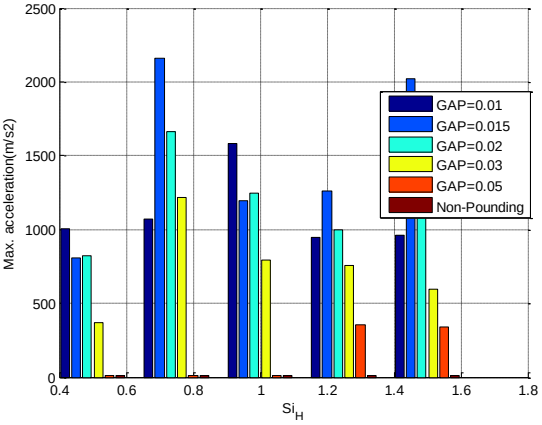


(c)

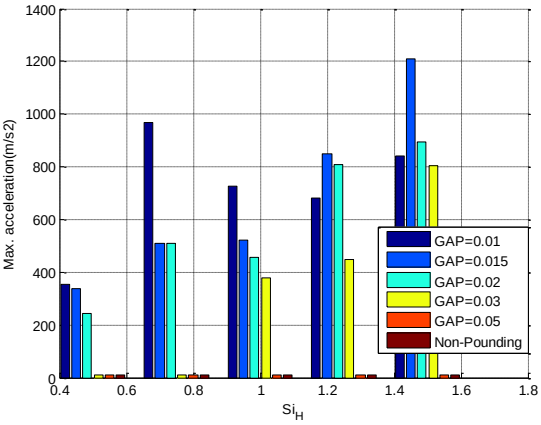


(d)

**Fig. 10:** The effects of $Si_H$ ratio on the maximum horizontal acceleration of right building with different separation gap: (a) Superstition, (b) Hachino, (c) El-Centro, (d) San Fernando

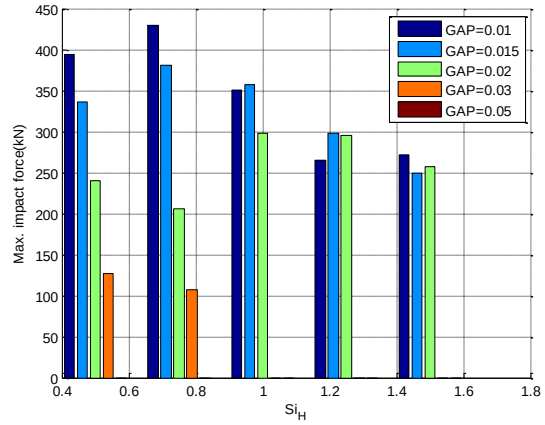


(a)

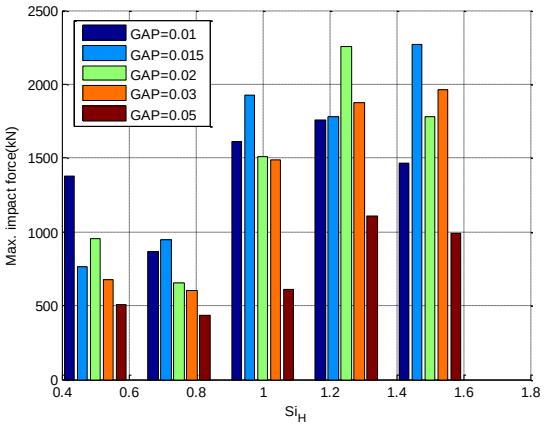


(b)

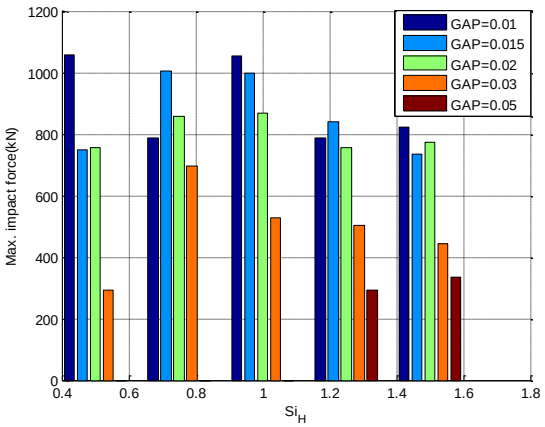


(c)

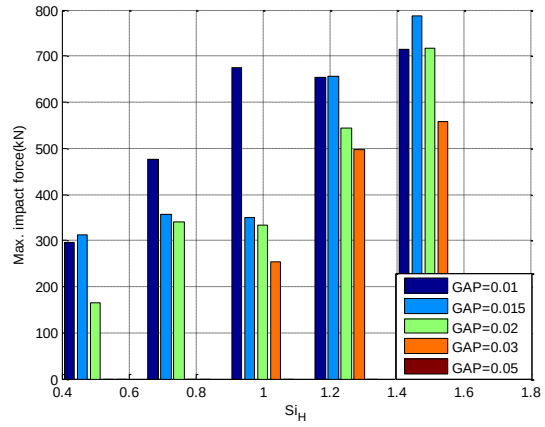


(d)

**Fig. 11:** The effects of $Si_H$ ratio on the maximum impact force of left building with different separation gap: (a) Superstition, (b) Hachino, (c) El-Centro, (d) San Fernando

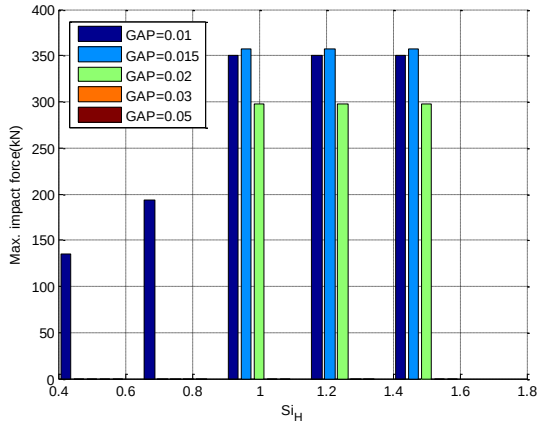


(a)

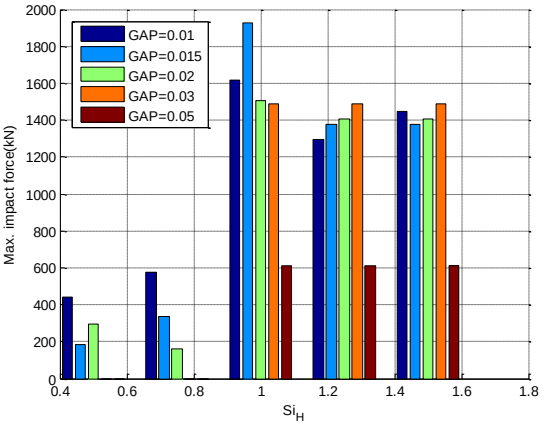


(b)

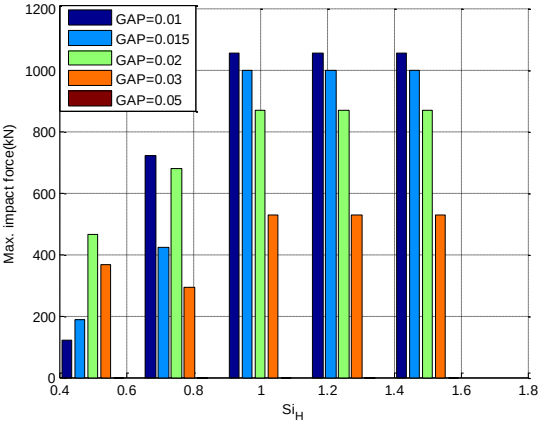


(c)

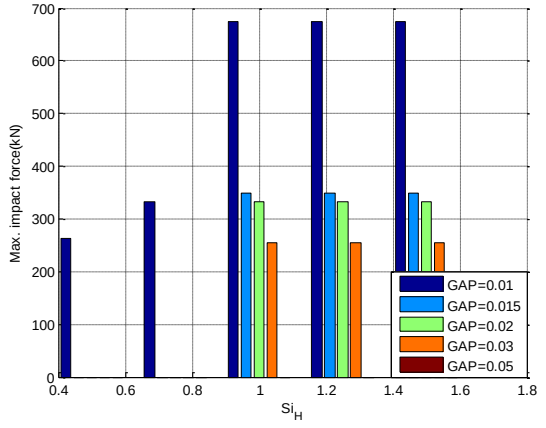


(d)

**Fig. 12:** The effects of $Si_H$ ratio on the maximum impact force of right building with different separation gap: (a) Superstition, (b) Hachino, (c) El-Centro, (d) San Fernando

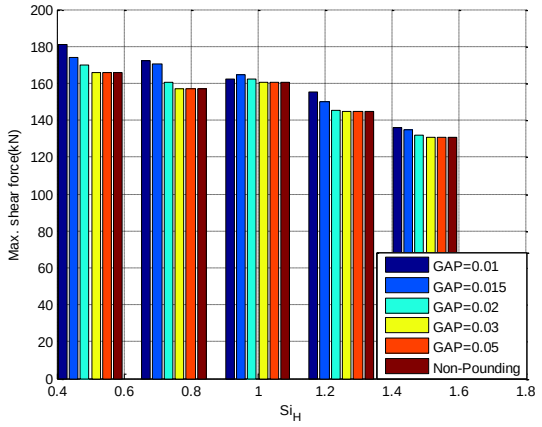


(a)

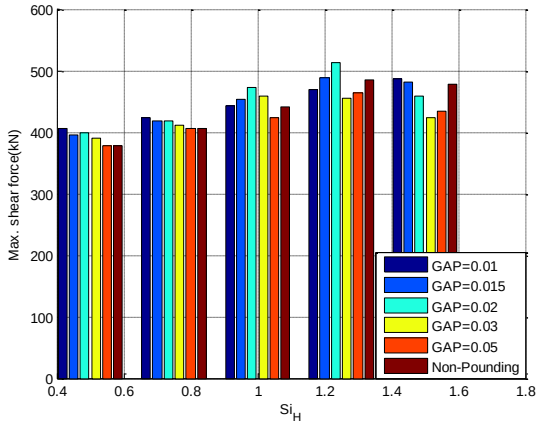


(b)

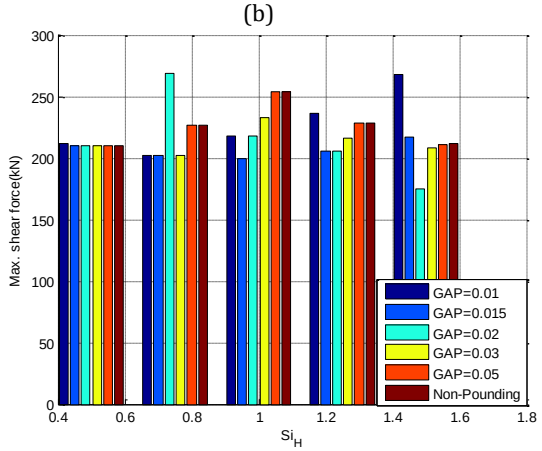


(c)

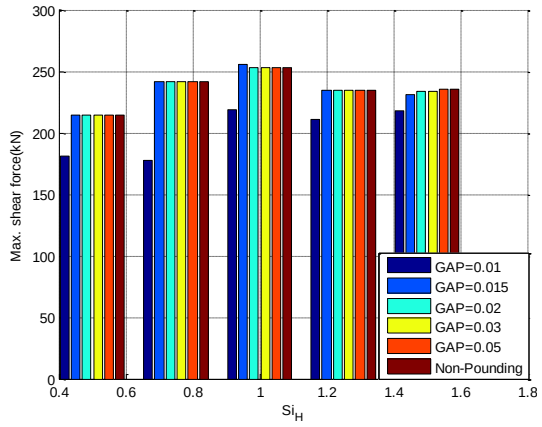


(d)

**Fig. 13:** The effects of $Si_H$ ratio on the maximum shear force of left building with different separation gap: (a) Superstition, (b) Hachino, (c) El-Centro, (d) San Fernando

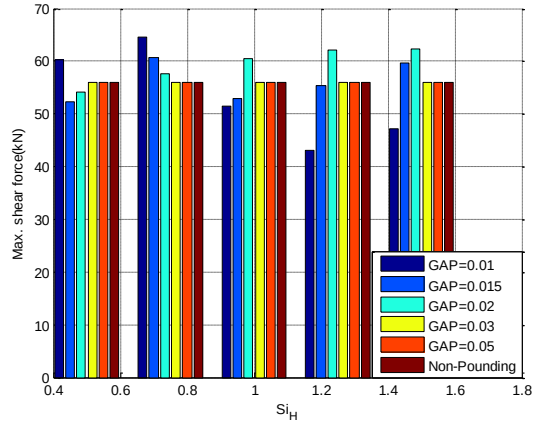


(a)

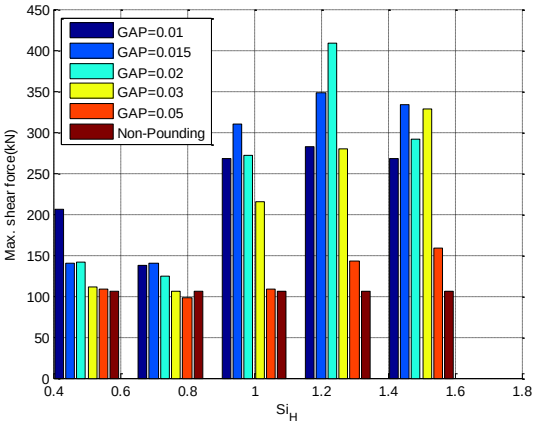


(b)

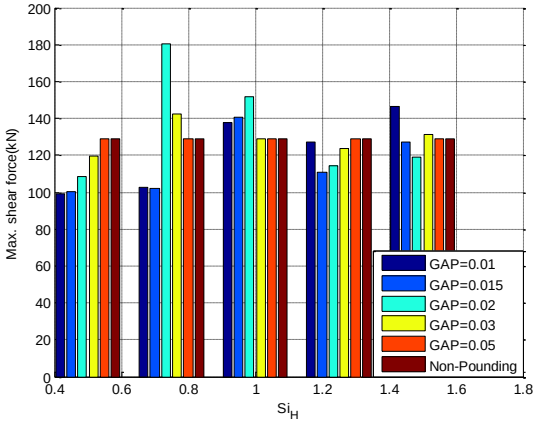


(c)

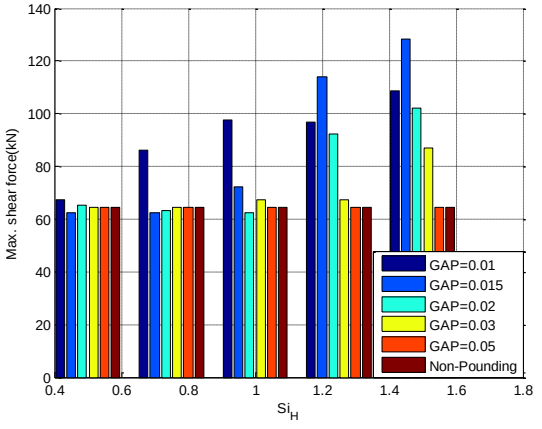


(d)

**Fig. 14:** The effects of $Si_H$ ratio on the maximum shear force of right building with different separation gap: (a) Superstition, (b) Hachino, (c) El-Centro, (d) San Fernando

Horizontal displacements depend on the motion acceleration, the dynamic characteristic of each structure, the separation gap, and the height ratio. For example, in the case of the Superstition earthquake and El-Centro earthquake, displacement and acceleration of the left building increase significantly when pounding was considered, as seen in Fig. 15, Fig. 17, and Fig. 19 (a and c). However, the opposite trend was observed in the right building, as being seen in Fig. 16, Fig. 18 and Fig. 20 (a and c).

On the other hand, pounding impact force opposing the motion of nodes will cause increases suddenly accelerations of nodes in each building. But, the increases are significant in the nodes around the top-point impact in both the structures due to the earthquakes with different parameters of the separation gap and the height ratio, see in Fig. 17 and Fig. 18.

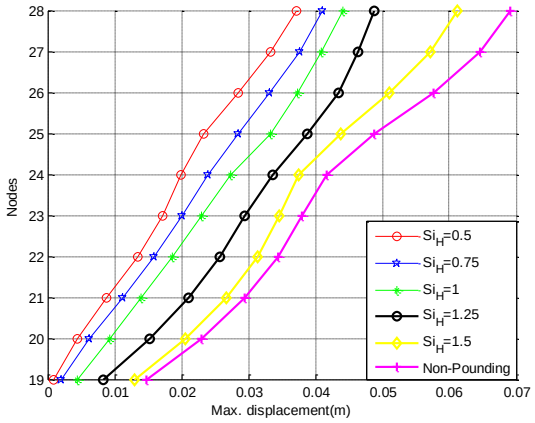


(d)

**Fig. 15:** The maximum horizontal displacement at node-frame of the left building with separation gap D=0.01 (m): (a) Superstition, (b) Hachino, (c) El-Centro, (d) San Fernando

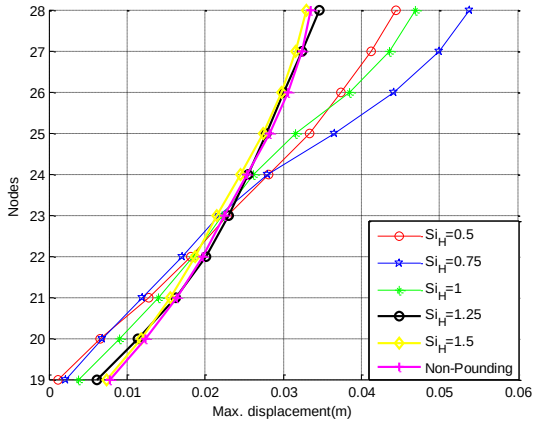


(a)

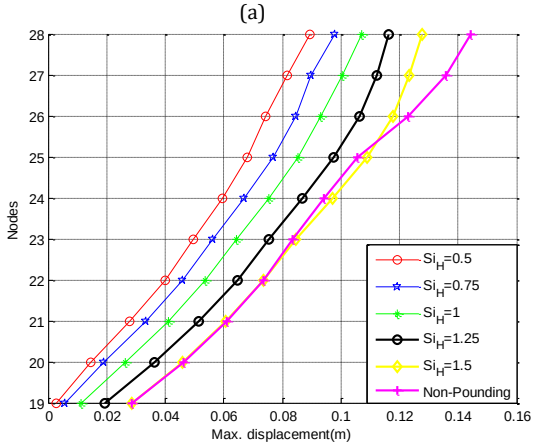


(b)

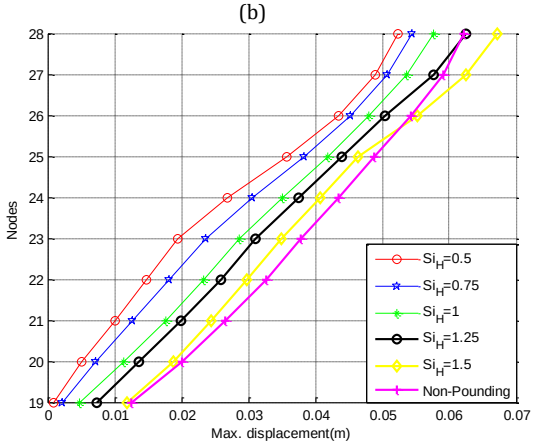


(c)

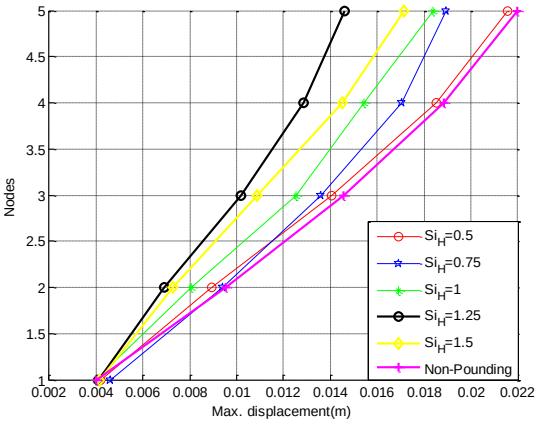


(a)

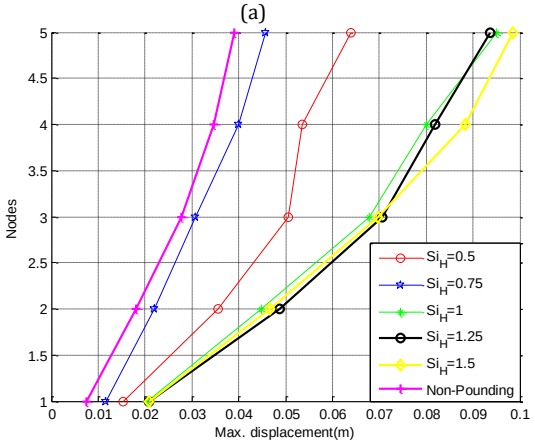


(b)

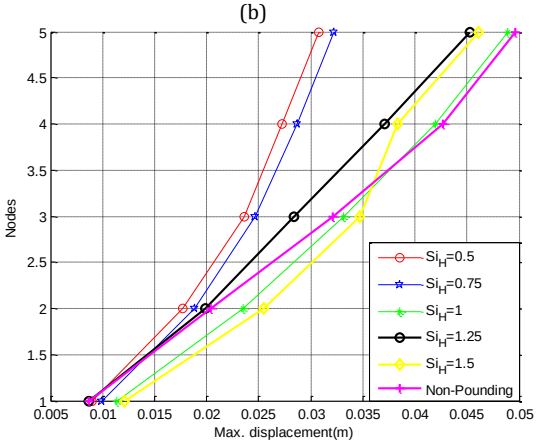


(c)

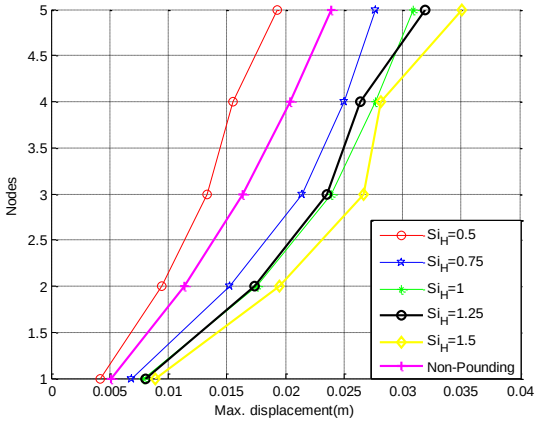


(d)

**Fig. 16:** The maximum horizontal displacement at node-frame of the right building with separation gap D=0.01 (m): (a) Superstition, (b) Hachino, (c) El-Centro, (d) San Fernando

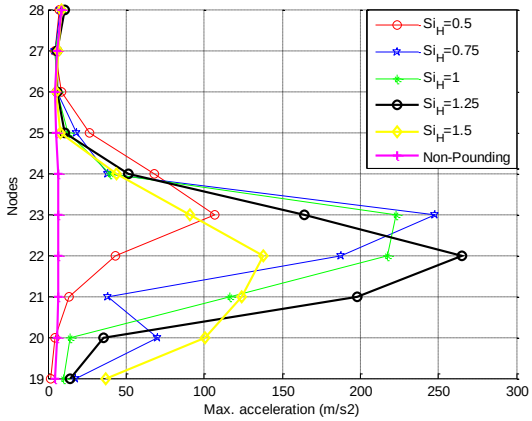


(d)

**Fig. 17:** The maximum horizontal acceleration at node-frame of the left building with separation gap D=0.01 (m): (a) Superstition, (b) Hachino, (c) El-Centro, (d) San Fernando

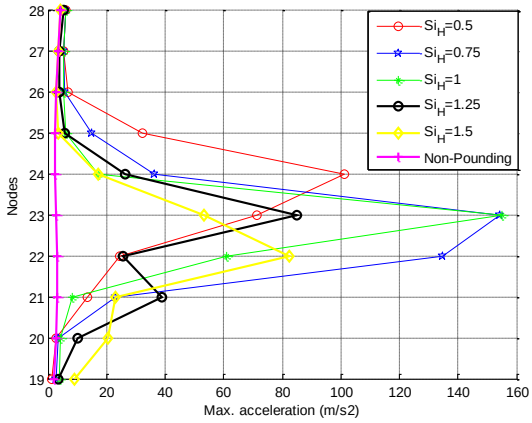


(a)

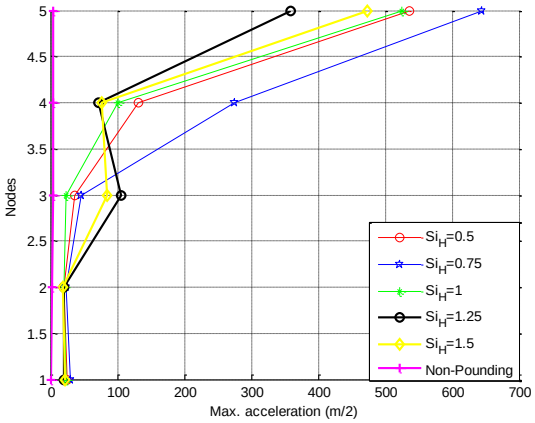


(a)

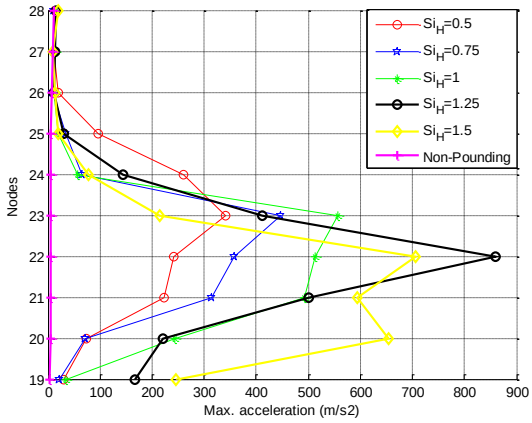


(b)

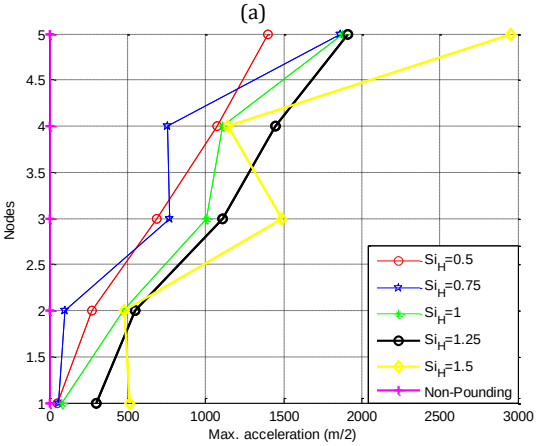


(b)

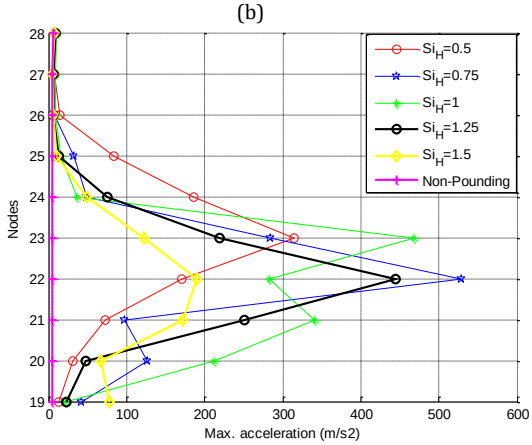


(c)

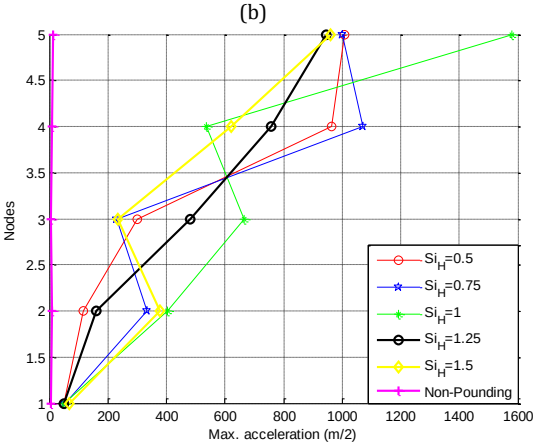


(c)

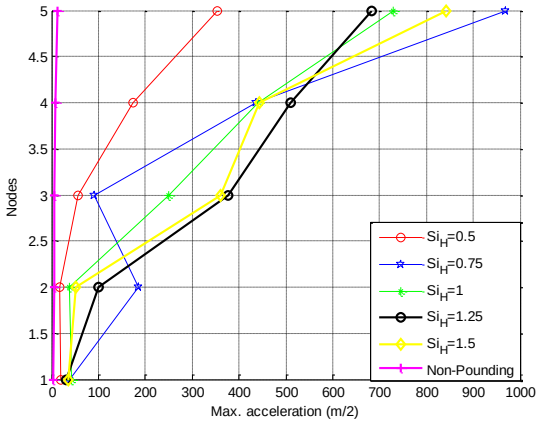


(d)

**Fig. 18:** The maximum horizontal acceleration at node-frame of the right building with separation gap D=0.01 (m): (a) Superstition, (b) Hachino, (c) El-Centro, (d) San Fernando

It can be explained that the impact forces at the nodes-impact at the top-point impact will be the largest (Fig. 19 and Fig. 20) because of the large deformation between together as mean as an increase impact force.

Additionally, an increase in the impact force will cause an increase in the drift horizontal displacement on each storey. Therefore, it is significantly increasing the shear force on columns of each storey of the system structure when the pounding effect was considered.

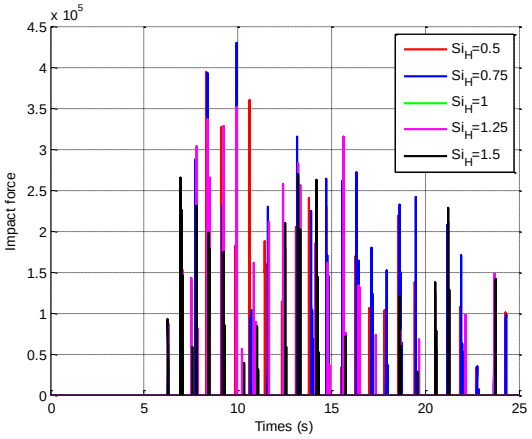


(a)

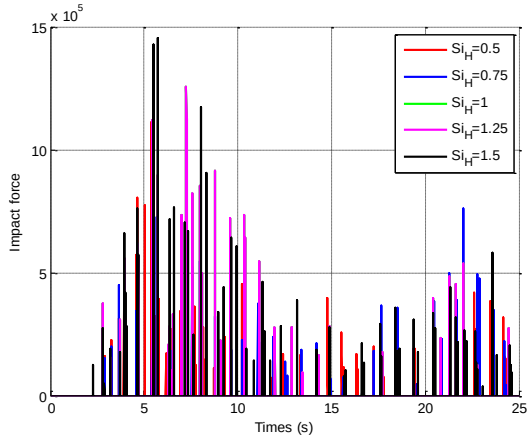


(b)

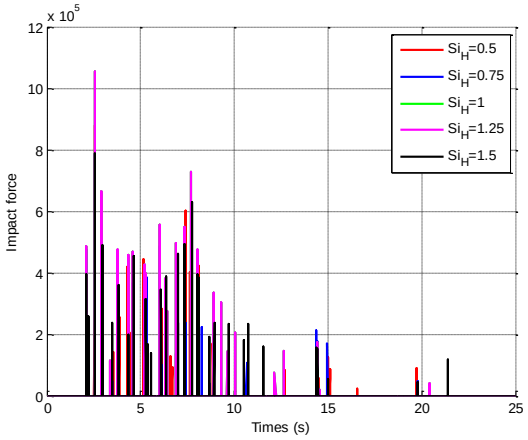


(c)

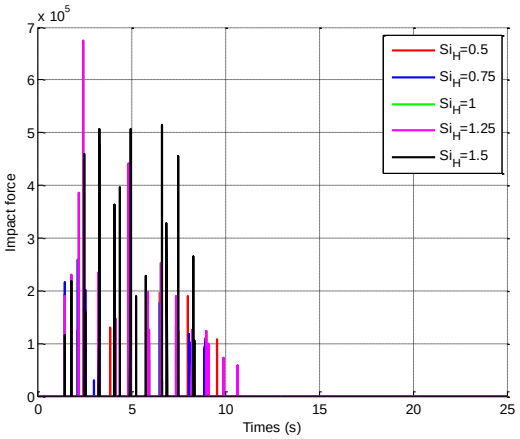


(d)

**Fig. 19:** The time history of impact force on the left building with separation gap D=0.01 (m): (a) Superstition, (b) Hachino, (c) El-Centro, (d) San Fernando

However, there is a difference in this case that the sheer force of columns, which are the nearest the top-node impact, the increases of the shear force are the largest, shown in Fig. 21 and Fig. 22. It can be seen that when the two adjacent structures occur the pounding effect due to earthquake excitations, the sheer force of the structures will increase suddenly, which is not as normal as the structures without consideration of the pounding effect. Hence, the effect is very dangerous for the general destruction of the building due to earthquake excitation. Besides, with an increase of the impact force will increase ability local destruction at nodes-impact, which lead to the general destruction of the system structure.

In the final investigation, the time history response of the structures due to the typical El-Centro earthquake is studied with separation gaps D = 0.01 and 0.03 (m). From Fig. 23 to Fig. 26 present the time history of horizontal displacement and acceleration at the top-nodes, respectively. The time history of the sheer force of the column element is presented in Fig. 27 and Fig. 28. It can be seen that pounding affect significantly on the time history dynamic response of the system structure due to earthquake excitations. The pounding impact force increases the probability of local destruction at an impact location between the two adjacent structures.

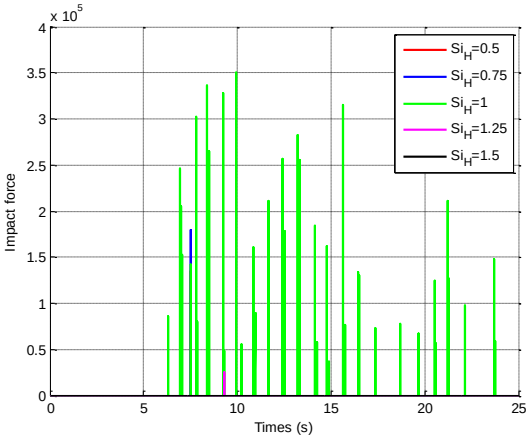


(a)

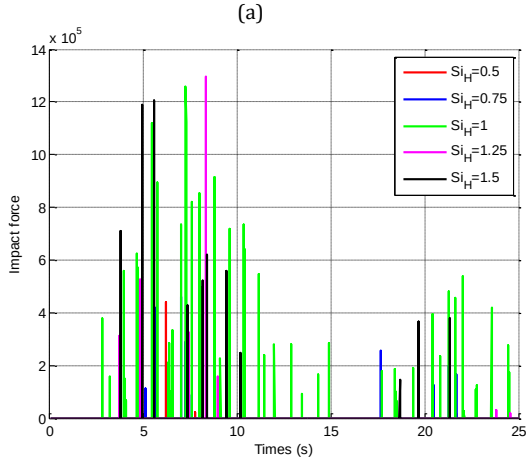


(b)

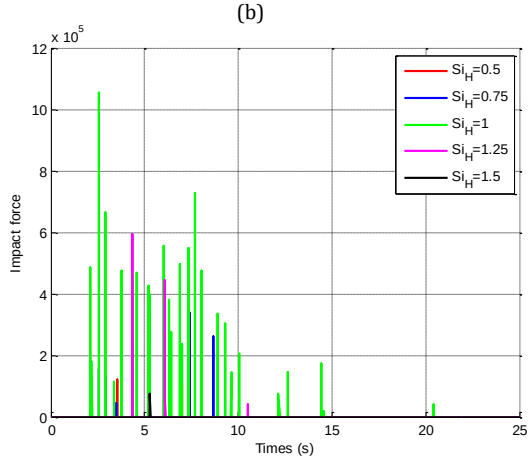


(c)

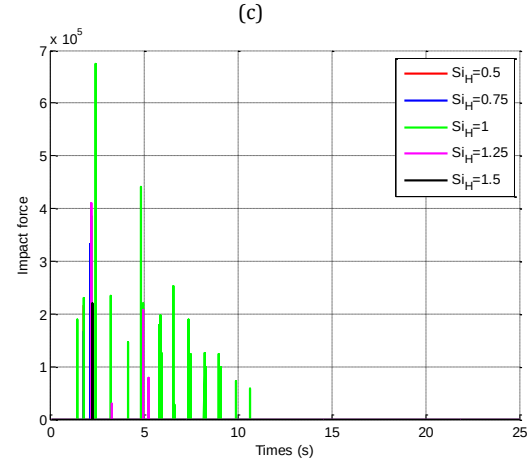


(d)

**Fig. 20:** The time history of impact force on the right building with separation gap D=0.01 (m): (a) Superstition, (b) Hachino, (c) El-Centro, (d) San Fernando

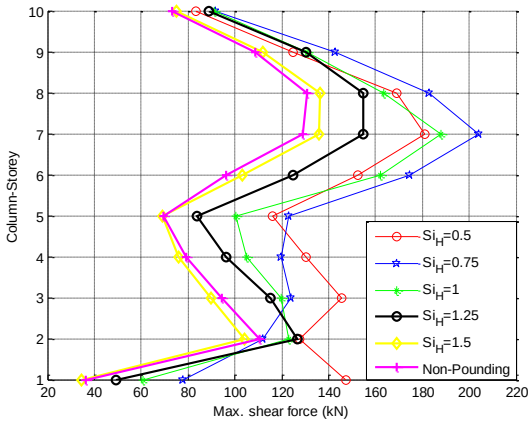


(a)

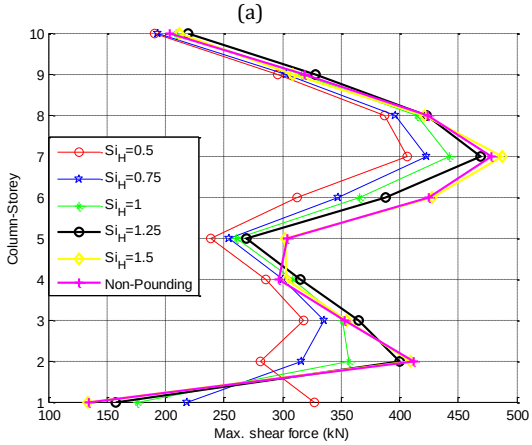


(b)

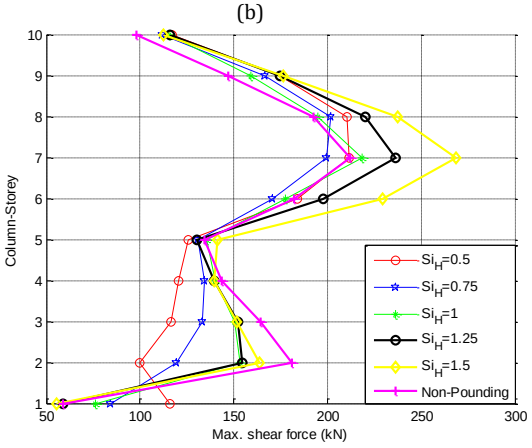


(c)

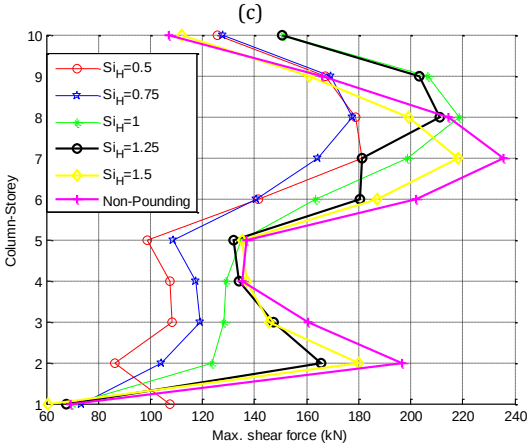


(d)

**Fig. 21:** The maximum sheer force of column-storey of the left building with separation gap D=0.01 (m): (a) Superstition, (b) Hachino, (c) El-Centro, (d) San Fernando

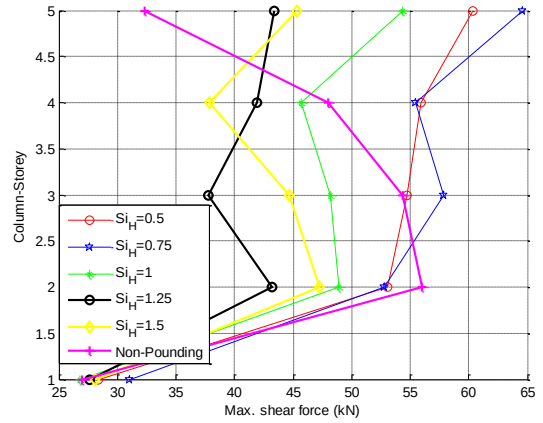


(a)

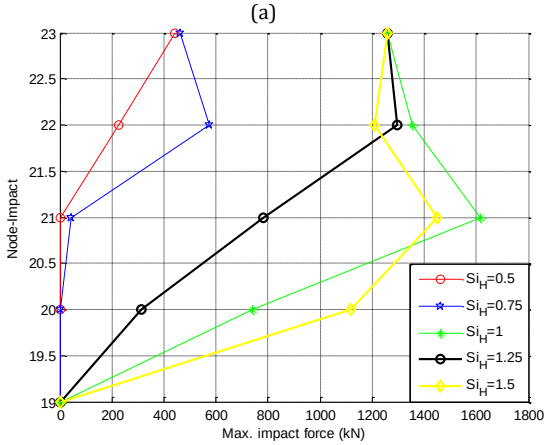


(b)

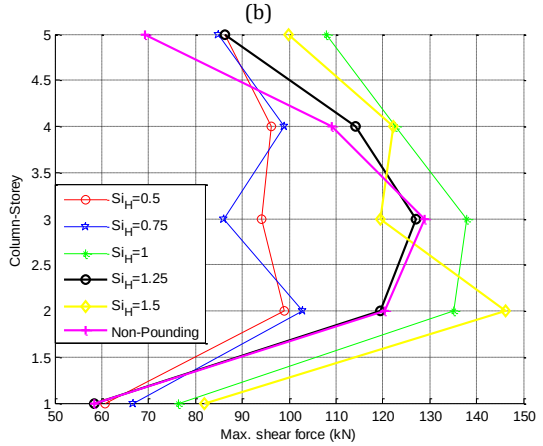


(c)

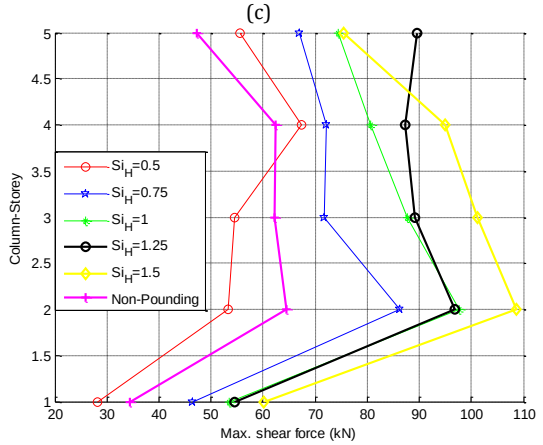


(d)

**Fig. 22:** The maximum sheer force of column-storey of the right building with separation gap D=0.01 (m): (a) Superstition, (b) Hachino, (c) El-Centro, (d) San Fernando

However, if the two adjacent structures have different floor levels, the impact forces concentrate near the mid-area of the column, which causes a buckling of the column. Therefore, it will also increase the general destruction of the buildings. It is noticed that with the same height ratio and the separation gap, a pounding effect on the dynamic response of the system structure is not the same for different earthquake excitations. Because the earthquake excitations will have different characteristic dynamics such as peak frequencies or amplitude of motion acceleration, hence, each of the dynamic characters of each structure combined with each the earthquake excitation and the property parameters of pounding will cause different influences on the dynamic response of the system structure. In most cases, the pounding effect increases significantly disadvantage to the dynamic response of the structures.

## 5. Conclusion

Based on the dynamic response of the two adjacent structures with different floor levels during an earthquake with pounding consideration, some important conclusions are drawn as follows:

- The formulation of the structure system of two adjacent structures with different floor levels during the earthquake was established to determine the effect of pounding on dynamic response. The height ratio $Si_H$, was proposed and investigated in different combinations of separation gaps and ground motions.
- The results showed that the pounding significantly affects the dynamic response of the structure system by increasing the peak accelerations and displacements.
- The numerical results also indicated that building with different height ratios experienced larger dynamic responses comparing to the case of equal floor levels during the earthquake. Therefore, it is recommended to build the two adjacent structures with the same floor level to minimize pounding during the earthquake.

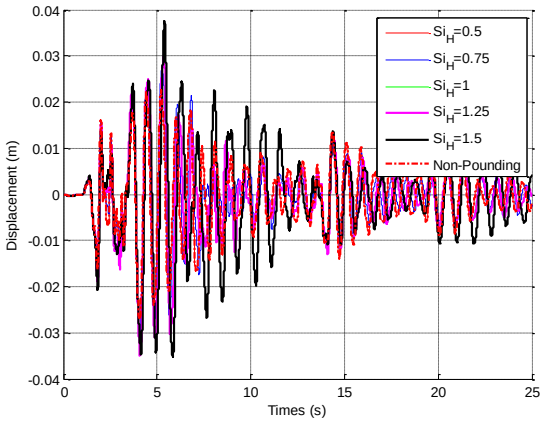


(a)

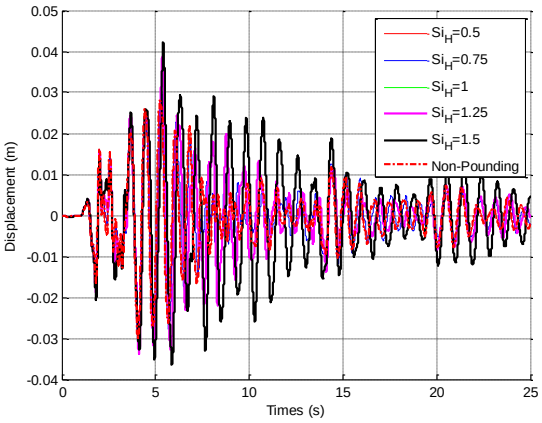


(b)

**Fig. 23:** The time history of horizontal displacement of the 24th node of the left building: (a) D=0.01 (m), (b) D=0.03 (m)

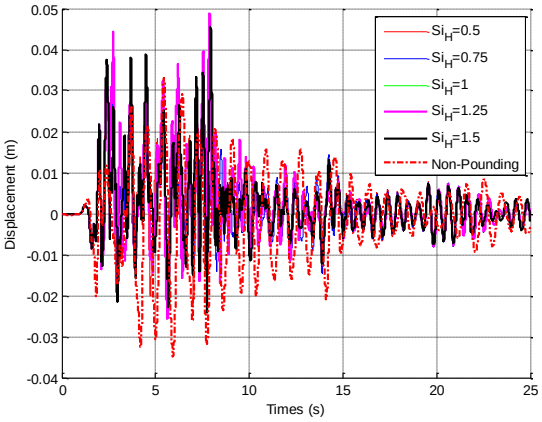


(a)

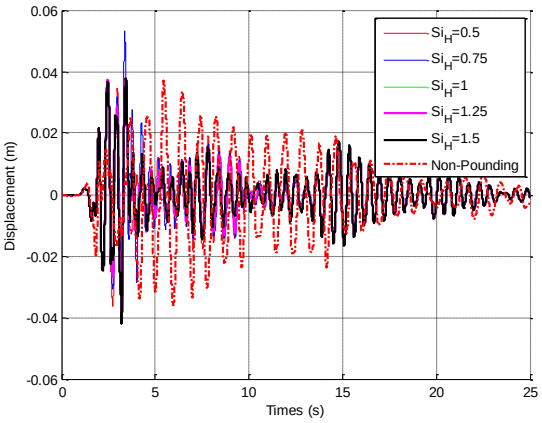


(b)

**Fig. 24:** The time history of horizontal displacement of the 6th node of the right building: (a) D=0.01 (m), (b) D=0.03 (m)

It can be confirmed that the paper analyzing the dynamic response of the two adjacent structures with different floor levels caused by earthquake-induced pounding can be considered as a meaningful practice problem. It has a complete agreement with narrow cities having high building density due to frequent earthquake excitations.

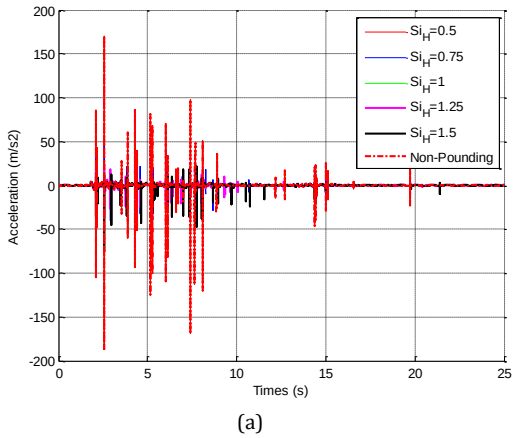


(a)

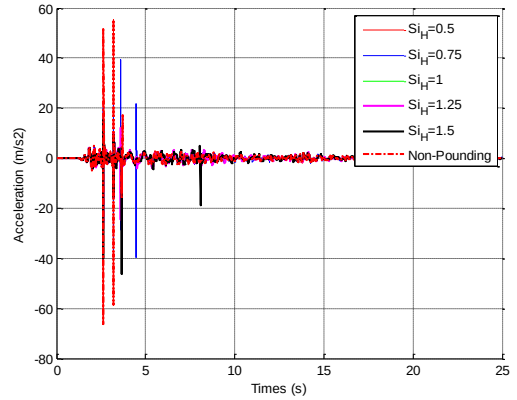


(b)

**Fig. 25:** The time history of horizontal acceleration of the 24th node of the left building: (a) D=0.01 (m), (b) D=0.03 (m)

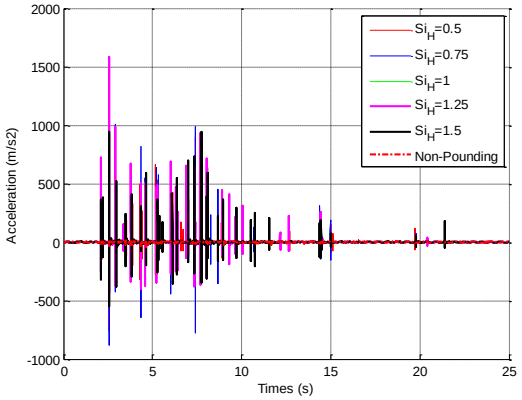


(a)

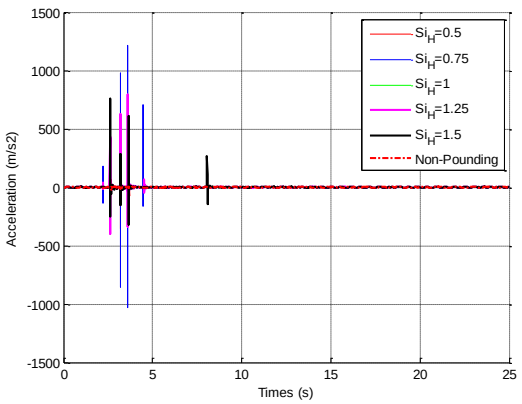


(b)

**Fig. 26:** The time history of horizontal acceleration of the 6thnode of the right building: (a) D=0.01 (m), (b) D=0.03 (m)

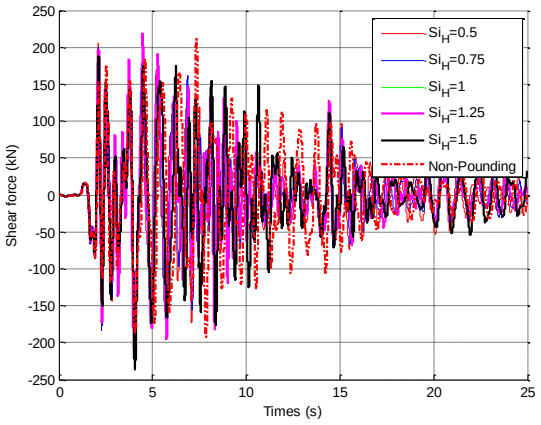


(a)

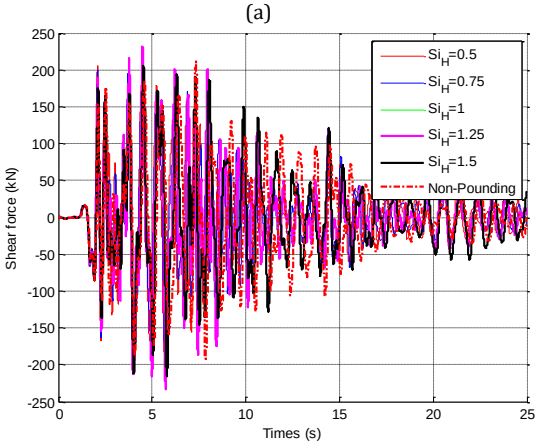


(b)

**Fig. 27:** The time history of sheer force of the 22nd element of the left building: (a) D=0.01 (m), (b) D=0.03 (m)

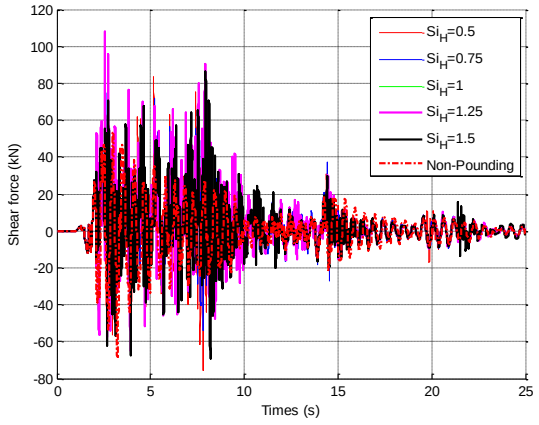


(a)

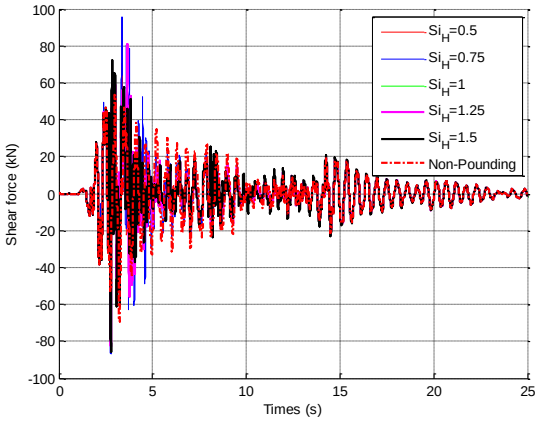


(b)

**Fig. 28:** The time history of sheer force of the 5th element of the right building: (a) D=0.01 (m), (b) D=0.03 (m)

## Compliance with ethical standards

## Conflict of interest

The authors declare that they have no conflict of interest.

## References

Agarwal VK, Niedzwecki JM, and Van de Lindt JW (2007). Earthquake induced pounding in friction varying base isolated buildings. Engineering Structures, 29(11): 2825-2832. https://doi.org/10.1016/j.engstruct.2007.01.026

Anagnostopoulos SA (1988). Pounding of buildings in series during earthquakes. Earthquake Engineering and Structural Dynamics, 16(3): 443-456. https://doi.org/10.1002/eqe.4290160311

Anagnostopoulos SA (1994). Earthquake induced pounding: State of the art. In the 10th European Conference on Earthquake Engineering, Rotterdam, Vienna, Austria, 2: 897-905.

Anagnostopoulos SA (2004). Equivalent viscous damping for modeling inelastic impacts in earthquake pounding problems. Earthquake Engineering and Structural Dynamics, 33(8): 897-902. https://doi.org/10.1002/eqe.377

Anagnostopoulos SA and Spiliopoulos KV (1992). An investigation of earthquake induced pounding between adjacent buildings. Earthquake Engineering and Structural Dynamics, 21(4): 289-302. https://doi.org/10.1002/eqe.4290210402

Chau KT, Wei XX, Shen CY, and Wang LX (2004). Experimental and theoretical simulations of seismic torsional poundings between two adjacent structures. In the 13th World Conference on Earthquake Engineering, Vancouver, Canada: 1-6.

Efraimiadou S, Hatzigeorgiou GD, and Beskos DE (2012). Structural pounding between adjacent buildings: the effects of different structures configurations and multiple earthquakes. In the 15th World Conference on Earthquake Engineering, Lisbon, Portugal: 24-28.

Efraimiadou S, Hatzigeorgiou GD, and Beskos DE (2013a). Structural pounding between adjacent buildings subjected to strong ground motions, Part I: The effect of different structures arrangement. Earthquake Engineering and Structural Dynamics, 42(10): 1509-1528. https://doi.org/10.1002/eqe.2285

Efraimiadou S, Hatzigeorgiou GD, and Beskos DE (2013b). Structural pounding between adjacent buildings subjected to strong ground motions, Part II: The effect of multiple earthquakes. Earthquake Engineering and Structural Dynamics, 42(10): 1529-1545. https://doi.org/10.1002/eqe.2284

Favvata MJ, Naoum MC, and Karayannis CG (2013). Earthquake induced interaction between RC frame and steel frame structures. WIT Transactions on the Built Environment, 134: 839-851. https://doi.org/10.2495/SAFE130741

Hameed A, Saleem M, Qazi AU, Saeed S, and Bashir MA (2012). Mitigation of seismic pounding between adjacent buildings. Pakistan Journal of Science, 64(4): 326-333.

Hatzigeorgiou GD and Pnevmatikos NG (2014). On the seismic response of collided structures. International Journal of Civil, Architectural, Structural and Construction Engineering, 8: 750-754.

Jankowski R (2005a). Impact force spectrum for damage assessment of earthquake-induced structural pounding. Key Engineering Materials, 293-294: 711-718.

https://doi.org/10.4028/www.scientific.net/KEM.293-294.711

Jankowski R (2005b). Non-linear viscoelastic modelling of earthquake-induced structural pounding. Earthquake Engineering and Structural Dynamics, 34(6): 595-611. https://doi.org/10.1002/eqe.434

Jankowski R (2006a). Analytical expression between the impact damping ratio and the coefficient of restitution in the non-linear viscoelastic model of structural pounding. Earthquake Engineering and Structural Dynamics, 35(4): 517-524. https://doi.org/10.1002/eqe.537

Jankowski R (2006b). Pounding force response spectrum under earthquake excitation. Engineering Structures, 28(8): 1149-1161. https://doi.org/10.1016/j.engstruct.2005.12.005

Jankowski R (2007). Assessment of damage due to earthquake-induced pounding between the main building and the stairway tower. Key Engineering Materials, 347: 339-344. https://doi.org/10.4028/www.scientific.net/KEM.347.339

Jankowski R (2008). Earthquake-induced pounding between equal height buildings with substantially different dynamic properties. Engineering Structures, 30(10): 2818-2829. https://doi.org/10.1016/j.engstruct.2008.03.006

Jankowski R (2010). Experimental study on earthquake-induced pounding between structural elements made of different building materials. Earthquake Engineering and Structural Dynamics, 39(3): 343-354. https://doi.org/10.1002/eqe.941

Jankowski R and Mahmoud S (2015). Earthquake-induced structural pounding. Springer International Publishing, Cham, Switzerland. https://doi.org/10.1007/978-3-319-16324-6

Karayannis CG and Favvata MJ (2005). Earthquake-induced interaction between adjacent reinforced concrete structures with non-equal heights. Earthquake Engineering and Structural Dynamics, 34(1): 1-20. https://doi.org/10.1002/eqe.398

Kasai K and Maison BF (1997). Building pounding damage during the 1989 Loma Prieta earthquake. Engineering Structures, 19(3): 195-207. https://doi.org/10.1016/S0141-0296(96)00082-X

Komodromos P, Polycarpou PC, Papaloizou L, and Phocas MC (2007). Response of seismically isolated buildings considering poundings. Earthquake Engineering and Structural Dynamics, 36(12): 1605-1622. https://doi.org/10.1002/eqe.692

Kumar P and Karuna S (2015). Effect of seismic pounding between adjacent buildings and mitigation measures. International Journal of Research in Engineering and Technology, 4(7): 208-216. https://doi.org/10.15623/ijret.2015.0407034

Li P, Liu S, and Lu Z (2017). Studies on pounding response considering structure-soil-structure interaction under seismic loads. Sustainability, 9(12): 2219. https://doi.org/10.3390/su9122219

Liu C, Yang W, Yan Z, Lu Z, and Luo N (2017). Base pounding model and response analysis of base-isolated structures under earthquake excitation. Applied Sciences, 7(12): 1238. https://doi.org/10.3390/app7121238

López-Almansa F and Kharazian A (2014). Parametric study of the pounding effect between adjacent RC buildings with aligned slabs. In the 2nd European Conference on Earthquake Engineering and Seismology: 15th European Conference on Earthquake Engineering, Istanbul, Turkey: 1-12.

Mahmoud S, Abd-Elhamed A, and Jankowski R (2013). Earthquake-induced pounding between equal height multi-storey buildings considering soil-structure interaction. Bulletin of Earthquake Engineering, 11(4): 1021-1048. https://doi.org/10.1007/s10518-012-9411-6

Mahmoud S, Austrell PE, and Jankowski R (2012). Simulation of the response of base-isolated buildings under earthquake excitations considering soil flexibility. Earthquake Engineering and Engineering Vibration, 11(3): 359-374. https://doi.org/10.1007/s11803-012-0127-z

Mattia L, Stefano S, and Gloria T (2015). Nonlinear modeling and mitigation of seismic pounding between RC frame buildings. Journal of Earthquake Engineering, 19(3): 431-460. https://doi.org/10.1080/13632469.2014.984370

Naderpour H, Barros RC, Khatami SM, and Jankowski R (2016). Numerical study on pounding between two adjacent buildings under earthquake excitation. Shock and Vibration, 2016: 1504783. https://doi.org/10.1155/2016/1504783

Namboothiri VP (2017). Seismic pounding of adjacent buildings. International Research Journal of Engineering and Technology, 4(3): 1443-1448.

Raheem SEA (2014). Mitigation measures for earthquake induced pounding effects on seismic performance of adjacent buildings. Bulletin of Earthquake Engineering, 12(4): 1705-1724. https://doi.org/10.1007/s10518-014-9592-2

Rosenblueth E and Meli R (1986). The 1985 Mexico earthquake. Concrete International, 8(5): 23-34.

Ruangrassamee A and Kawashima K (2001). Relative displacement response spectra with pounding effect. Earthquake Engineering and Structural Dynamics, 30(10): 1511-1538. https://doi.org/10.1002/eqe.75

Trung PD, Quang PT, Toan NB, Hoa HP, and Phuoc NT (2018). The effectiveness of rubber absorber in adjacent planar structures under earthquake-included pounding. International Journal of Civil Engineering and Technology, 9(8): 1751-1768.

Tubaldi E, Barbato M, and Ghazizadeh S (2012). A probabilistic performance-based risk assessment approach for seismic pounding with efficient application to linear systems. Structural Safety, 36: 14-22. https://doi.org/10.1016/j.strusafe.2012.01.002